

Identification of invalid time-delay-groups using discriminant and Jacobian-determinant in acoustic emission PD source localisation

ISSN 1751-8822
 Received on 31st August 2016
 Revised 27th October 2016
 Accepted on 22nd November 2016
 E-First on 18th January 2017
 doi: 10.1049/iet-smt.2016.0362
 www.ietdl.org

Deepthi Antony¹, Gururaj S. Punekar¹ ✉

¹Electrical and Electronics Department, National Institute of Technology, Surathkal, Karnataka, India

✉ E-mail: gsp@nitk.ac.in

Abstract: The key problem in locating a source of partial discharge (PD) using the acoustic emission technique is the error in estimating the signal arrival time from the source to the multiple sensors. When the time difference of arrival approach is used for the PD-source-localisation, some of the measured time-delay-groups will have solution for the time-difference equation in the complex-number-field. This is due to the significant error in the arrival time estimation. Such time-delay-groups should be considered to be invalid. In this study, a function is proposed for identifying the invalid time-delay-groups for the fixed set of coordinates of four sensors and the specific velocity of the acoustic signal used. The negative sign of this function value indicates that the solution is in the complex-number-field. An alternative method for identifying the invalid time-delay-groups is by using Newton's method. The multiple sign changes of the Jacobian-determinant in the iterations of Newton's method shows that the solution is in the complex-number-field. The proposed methods have been tested with data from the existing literature, and results have confirmed the efficacy of these methods in the identification of the invalid time-delay-groups. Discarding such groups of time delays improves the accuracy of statistical PD-source-localisation.

1 Introduction

Partial discharge (PD) measurements play a very important role in the electrical quality control testing of high voltage (HV) apparatus that employs a composite insulation. In power transformers, PDs are both a symptom and a cause of deterioration [1]. PDs are pulse-like in nature and they result in the emission of acoustic signals. Acoustic emissions (AEs) are phenomena whereby transient elastic waves are generated by the rapid release of energy from the localised sources within a material [2]. These acoustic waves propagate within the transformer. AEPD detection technology, while being non-invasive, is widely used for online PD detection in power transformers. The ability to locate the source of PD, and also its immunity to electromagnetic interference, is vital under field conditions [3, 4]. The cost that is incurred due to transformer failure can be reduced by an early detection and a localisation of the PDs [5].

The de-noising of signals that are obtained from the AE sensors is essential, as extensive noise coupled with measured signals can cause ambiguities in the PD-source-localisation [6–8]. The measurement of signals in the ultra-high-frequency (UHF) range is advantageous for a noise-immune analysis, as it is carried out in an electromagnetically clean enclosure of an HV apparatus [9]. However, the UHF detection technique uses oil filtration valves for the sensor insertion, and is thus invasive. The other major issue with UHF detection is the calibration capability of this measuring method [10, 11]. In the case of a PD detection when using AE signals, the considerably slow propagation velocity of the acoustic waves inside the transformer allow for a better signal arrival time measurement [12]. False indications of a PD can be minimised with the AE noise reduction. This can be achieved based on PD pattern recognition, the time- and frequency-domain characteristics, and a pulse time-of-flight analysis. The PD pattern identification is an important tool in identifying the type of a PD defect [13–16]. The AE sensor recordings help in distinguishing between the different PD types which are related to the insulation failure [17–20].

The present study has dealt with the issues that are associated with the AEPD-source-localisation. The geometrical localisation of a PD can be achieved by using the time difference of arrival (TDOA) approach. In the TDOA approach, multiple sensors are

placed on the transformer's tank wall [21]. The sensor nearest to the PD source receives signals first. Then a recording process is triggered on all of the sensors simultaneously. The time delay in the signal reception of the other sensors, with respect to the nearest sensor, is measured.

The time-difference equations (non-linear sphere equations) are formed by considering each sensor as being the centre of the sphere. The radius of this sphere is the distance between the sensor and the PD source. The spheres intersect with each other at the PD location. The coordinates of the PD source (x, y, z) and the arrival time of the acoustic signal to the nearest sensor (T) are the unknown quantities. Since there are four unknowns, a minimum of four sensors are required in order to locate the PD source. A system of non-linear sphere equations is given in (1): where (x_n, y_n, z_n) , for $n = 1$ to 4, form the coordinates of the four sensors, ' v ' is the specific velocity of the acoustic signal [2], and t_{12}, t_{13} , and t_{14} are the time delays in the signal reception of the other sensors, with respect to the nearest sensor [22]

$$\begin{aligned}
 (x - x_1)^2 + (y - y_1)^2 + (z - z_1)^2 &= (vT_1)^2 \\
 (x - x_2)^2 + (y - y_2)^2 + (z - z_2)^2 &= \{v(T_1 + t_{12})\}^2 \\
 (x - x_3)^2 + (y - y_3)^2 + (z - z_3)^2 &= \{v(T_1 + t_{13})\}^2 \\
 (x - x_4)^2 + (y - y_4)^2 + (z - z_4)^2 &= \{v(T_1 + t_{14})\}^2
 \end{aligned} \tag{1}$$

In PD-source-localisation (using a fixed set of coordinates for the four sensors and the specific velocity of an acoustic signal), the normal practise is to acquire many groups of signals and measure the corresponding time delays [23]. The time delays: namely, t_{12}, t_{13} , and t_{14} form one group. Each such group of time delays give the location of the PD source. In general, the mean value of these locations gives the statistical location of the PD source [23].

The key problem in locating the PD source by using the AE technique is the error in this time-delay measurement. Estimating time delays accurately is difficult due to the noise and the initial oscillation of the acquired AE burst signals [24]. The acoustic wave attenuation and the transit time are extremely sensitive to the conditions of the medium in which they propagate [25]. The acoustic velocity in transformer oil is not constant, but it depends

on a complex relationship including the temperature of the oil, its gas content, the moisture content, and also the frequency content of the propagating signal [26].

The bias errors can be caused due to a sensor fault, a sensor ageing, or the proximity of the PD to a certain sensor when in comparison with the other sensors. If any sensor acquires a large bias error in the measurement of the time delays, a convergence problem is to be expected in the algorithms that were used for the PD-source-localisation [27]. The errors in a time-delay measurement are sometimes so significant that there is 'no-solution' to the time-difference equations in the real-number-field. Hence, by identifying and discarding the time-delay-groups, which result in a solution of the system of non-linear equations in the complex-number-field, would be advantageous in improving the accuracy of PD-source-localisation.

Irrespective of the algorithm that was used for PD-source-localisation, if the measured time delays are inaccurate, there will be a significant error in the detected PD-source location. The methods for mathematically identifying the invalid 'time-delay-groups' is the contribution of this paper. This proposed method is also applicable to UHF signals in a PD-source-localisation. The proposed methods will have an even greater significance with an UHF-based PD-source-localisation where estimated time delays are in the range of nanoseconds.

2 Identification of invalid time-delay-groups

A PD source is located by solving the system of the non-linear sphere equations. The intersection of any two spheres (out of four) forms a plane. The PD source can be located on this intersecting plane. Two such planes intersect in a line. The PD source can be located on this line. The line intersects any one of the spheres in two points. This results in a quadratic equation [24]. One of the solutions of this quadratic equation is the PD-source location. If the quadratic equation does not have a real solution, it implies that the measured time-delay-group has a significant error. The function given in (21) is derived on the basis that the nature of the roots of the quadratic equation can be identified from the discriminant value. The SI unit for the given function is square metres. The constants σ_1 – σ_{19} given in (2)–(20) are determined by using known quantities such as the coordinates of the sensor, the velocity of the acoustic signal, together with the measured time delays. These constants are used to find the function value given in (21). The derivation of the function (21) and the associated constants (2)–(20) are shown in the Appendix. However, for a measured time-delay-group, if the function value is negative, the PD source that is located by using those time delays will be in the complex-number-field. Such groups of time delays should be considered to be invalid and discarded

$$\sigma_1 = \frac{(x_1 - x_2)}{2t_{12}v^2} - \frac{(x_1 - x_3)}{2t_{13}v^2} \quad (2)$$

$$\sigma_2 = \frac{(x_1 - x_2)}{2t_{12}v^2} - \frac{(x_1 - x_4)}{2t_{14}v^2} \quad (3)$$

$$\sigma_3 = \frac{(y_1 - y_2)}{2t_{12}v^2} - \frac{(y_1 - y_3)}{2t_{13}v^2} \quad (4)$$

$$\sigma_4 = \frac{(y_1 - y_2)}{2t_{12}v^2} - \frac{(y_1 - y_4)}{2t_{14}v^2} \quad (5)$$

$$\sigma_5 = \frac{(z_1 - z_2)}{2t_{12}v^2} - \frac{(z_1 - z_3)}{2t_{13}v^2} \quad (6)$$

$$\sigma_6 = \frac{(z_1 - z_2)}{2t_{12}v^2} - \frac{(z_1 - z_4)}{2t_{14}v^2} \quad (7)$$

$$\sigma_7 = \frac{t_{12}^2v^2 + x_1^2 - x_2^2 + y_1^2 - y_2^2 + z_1^2 - z_2^2}{2t_{12}v^2} \quad (8)$$

$$\sigma_8 = \sigma_7 - \frac{t_{13}^2v^2 + x_1^2 - x_3^2 + y_1^2 - y_3^2 + z_1^2 - z_3^2}{2t_{13}v^2} \quad (9)$$

$$\sigma_9 = \sigma_7 - \frac{t_{14}^2v^2 + x_1^2 - x_4^2 + y_1^2 - y_4^2 + z_1^2 - z_4^2}{2t_{14}v^2} \quad (10)$$

$$\sigma_{10} = \sigma_1\sigma_6 - \sigma_2\sigma_5 \quad (11)$$

$$\sigma_{11} = \sigma_3\sigma_6 - \sigma_4\sigma_5 \quad (12)$$

$$\sigma_{12} = \sigma_1\sigma_4 - \sigma_2\sigma_3 \quad (13)$$

$$\sigma_{13} = \sigma_2\sigma_8 - \sigma_1\sigma_9 \quad (14)$$

$$\sigma_{14} = \sigma_4\sigma_8 - \sigma_3\sigma_9 \quad (15)$$

$$\sigma_{15} = 2(\sigma_1\sigma_4 - \sigma_2\sigma_3) \quad (16)$$

$$\sigma_{16} = z_1 - z_2 - \frac{\sigma_{10}(y_1 - y_2)}{\sigma_{12}} + \frac{\sigma_{11}(x_1 - x_2)}{\sigma_{12}} \quad (17)$$

$$\sigma_{17} = t_{12}^2v^2 + x_1^2 - x_2^2 + y_1^2 - y_2^2 + z_1^2 - z_2^2 + \frac{2\sigma_{13}(y_1 - y_2)}{\sigma_{15}} - \frac{2\sigma_{14}(x_1 - x_2)}{\sigma_{15}} \quad (18)$$

$$\sigma_{18} = y_1 + \frac{\sigma_{13}}{\sigma_{15}} \quad (19)$$

$$\sigma_{19} = x_1 - \frac{\sigma_{14}}{\sigma_{15}} \quad (20)$$

$$F = \left[2z_1 - \frac{2\sigma_{10}\sigma_{18}}{\sigma_{12}} + \frac{2\sigma_{11}\sigma_{19}}{\sigma_{12}} - \frac{\sigma_{16}\sigma_{17}}{t_{12}^2v^2} \right]^2 - \left[\sigma_{18}^2 + \sigma_{19}^2 + z_1^2 - \frac{\sigma_{17}^2}{4t_{12}^2v^2} \right] \left[4\left(\frac{\sigma_{10}}{\sigma_{12}}\right)^2 + 4\left(\frac{\sigma_{11}}{\sigma_{12}}\right)^2 - \frac{4\sigma_{16}^2}{t_{12}^2v^2} + 4 \right] \quad (21)$$

The system of non-linear equation can be solved by using Newton's method [28]. An alternative method for identifying the invalid time-delay-groups is by solving the system of the non-linear equations by using Newton's method. A detailed flowchart for the identification of the invalid time-delay-group by using Newton's method (including the proposed extension of Newton's method for the identification of invalid time-delay-groups) is shown in Fig. 1. When a system has complex roots, a straight line solution no longer exists. The solution either spiral toward or spiral away from the origin [29]. Any sign transition of the eigenvalues is reflected in the sign change of the Jacobian-determinant. From a computational point of view monitoring the sign changes of all the eigenvalues are quite difficult. Therefore, an alternative and efficient method is to monitor the sign changes of Jacobian-determinant [30]. Hence in the present study, the sign of the Jacobian-determinant is checked for all iterations of Newton's method. This is indicated in Fig. 1 by highlighting this part in the flowchart. If the sign (+ve or -ve) of the determinant value changes from one iteration to the next, multiple times, it shows a clear case of oscillation. These oscillations are attributed to the non-convergence of Newton's method, due to an unavailability of a real solution. In some special cases, when the PD source is equidistant from the sensors or when all x , all y , or all z coordinates of the sensors are the same, some of the constants listed in (2)–(20) cannot be found (NaN). Hence, the function value cannot be determined. In such cases, the invalid time-delay-groups can be identified by this proposed alternative method involving Newton's algorithm.

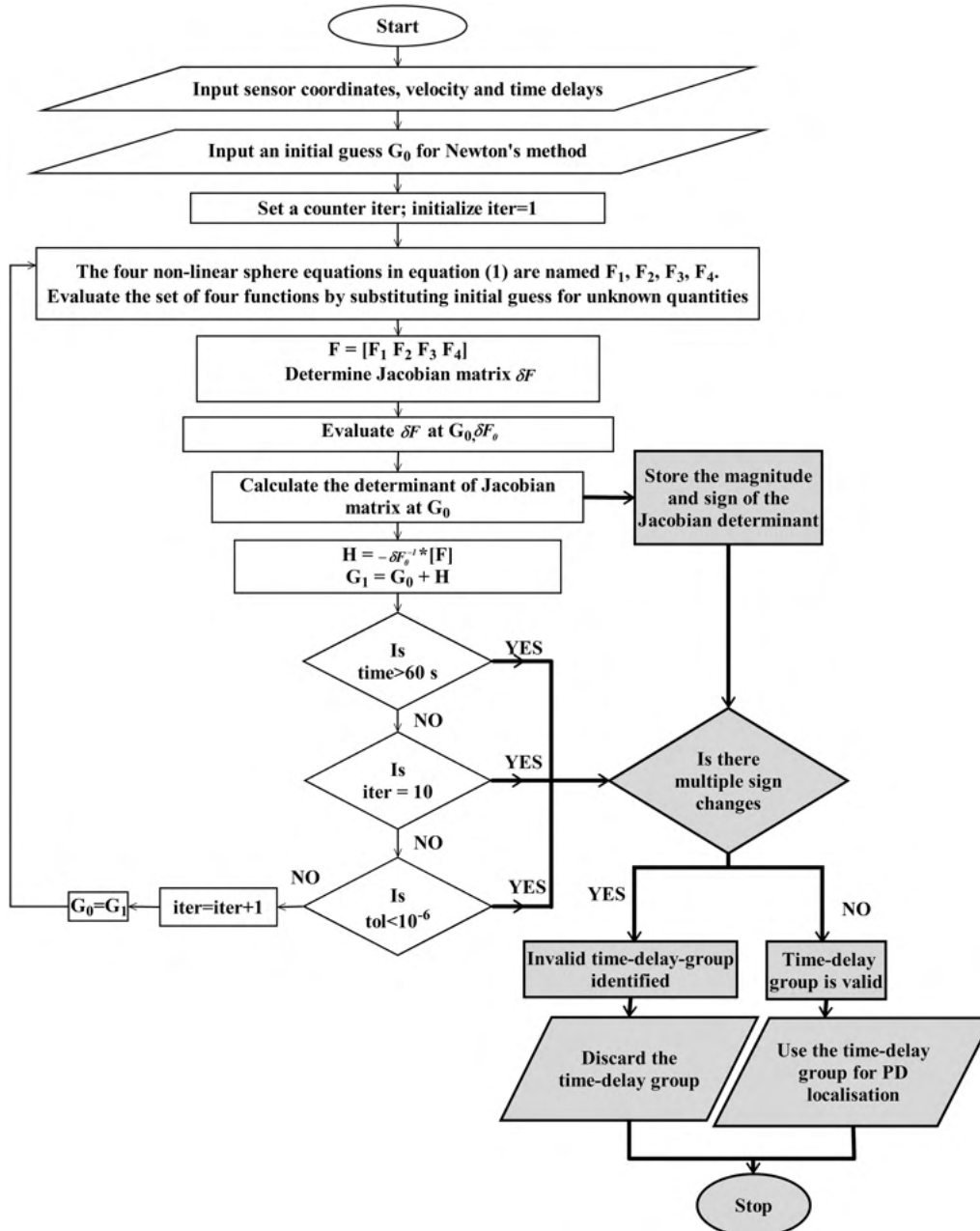


Fig. 1 Flowchart for identification of invalid time-delay-group by using Newton's method (The highlighted portion is the proposed extension of Newton's method for the identification of invalid time-delay-group.)

3 Results and discussion

To validate the proposed methods with practical data, the data from [21] are taken and analysed. The experimental setup used in [21] consists of a lidless transformer tank of size $120 \times 80 \times 100 \text{ cm}^3$. The tank is filled with oil, in which a needle-to-back electrode is mounted (transformer insulating paper is inserted between the needle and the back). The acoustic signals are generated when the voltage is raised to 50 kV. The measurements were carried out at a test oil temperature of 25°C . The propagation velocity of the acoustic signal in oil at 25°C is found to be 1400 m/s. Four acoustic sensors are mounted on the transformer tank. The coordinates of the four sensors are S_1 (80, 82, 36.5), S_2 (24.5, 0, 34.3), S_3 (0, 60, 38.5), and S_4 (32, 120, 23) cm. The experiments are conducted for two different PD sites. The coordinates of the two PD sites are PD1 (58.5, 61, 24.2) and PD2 (70, 43, 52) cm.

In this paper, one of the PD-source locations (of the two), with coordinates of (70, 43, 52) cm, is chosen for the analysis. Table 1 shows the five groups of time delays that were measured (TD-1–TD-5) for the corresponding PD-source location, as given in [21]. The function value found by using (21) for each time-delay-group is also shown in Table 1. Newton's method is implemented in order

to solve the system of the non-linear equations, with an initial guess of (0, 0, 0, 0) for (x, y, z, T) . For each time-delay-group, the Jacobian-determinants for ten iterations of Newton's method are given in Table 2. From Tables 1 and 2, it can be seen that for the time-delay-group which has a negative function value, the Jacobian-determinant changes its sign multiple times. This indicates that the corresponding time-delay-group that is measured will result in complex solution for the system of the non-linear equations. Whenever the function value [of (21)] is positive, the determinant will converge to a fixed value with at most one sign change. This indicates that the system has a real solution.

From Tables 1 and 2, it can be observed that the two groups of time delays that resulted in a negative function value and an oscillation of the Jacobian-determinant are TD-3 and TD-4. The theoretical time-delay-group for the considered PD source is (110, 223, 334) μs [21]. The percentage errors in the measured time delays for TD-3 and TD-4 are calculated using (22) and they are shown in Table 3. From Table 3, it can be seen that the measured time delay has a significant error

Table 1 Time-delay-groups given in [21] and corresponding function value computed for each time-delay-group

Time-delay-groups	$t_{12}, \mu\text{s}$	$t_{13}, \mu\text{s}$	$t_{14}, \mu\text{s}$	Function value, cm^2 [from (21)]
TD-1	82	250	374	3.02×10^{-1}
TD-2	131	200	321	2.84×10^{-1}
TD-3	145	207	351	-1.54×10^{-1}
TD-4	93	191	345	-4.01×10^{-2}
TD-5	206	358	253	2.12×10^3

Table 2 Jacobian-determinants calculated for ten iterations in Newton's method for each time-delay-group (TD-1–TD-5)

Iteration number	TD-1	TD-2	TD-3	TD-4	TD-5
1	-1399.6	-1717.8	-1957.3	-1640.1	-952.38
2	-1600.7	-2120.1	-2234.4	-1922.8	-929.33
3	-956.80	-1238.4	-991.42	-932.15	-3060.5
4	-740.15	-924.57	-212.17	-405.75	-2318.5
5	-708.44	-871.30	+1218.8	-64.290	-2199.7
6	-707.73	-869.67	+378.77	+842.45	-2196.5
7	-707.73	-869.67	-552.76	+354.47	-2196.5
8	-707.73	-869.67	+232.16	+18.610	-2196.5
9	-707.73	-869.67	-1094.7	-3011.9	-2196.5
10	-707.73	-869.67	-290.60	-1487.3	-2196.5

Table 3 Percentage error in time delay in time-delay-groups TD-3 and TD-4

Group	Percentage error		
	t_{12}	t_{13}	t_{14}
TD-3	+31.82	-7.170	+5.090
TD-4	-15.45	-14.35	+3.290

Table 4 PD source located using different algorithms with time-delay-groups TD-3 and TD-4

Algorithm	PD coordinates, cm					
	X	TD-3 Y	Z	X	TD-4 Y	Z
non-iterative method	$69 + 5i$	$42 - i$	$59 + 25i$	$73 + 3i$	$35 - i$	$67 + 14i$
Newton's method	656	-5	259	88	30	125
least-square algorithm	a	a	a	69.1	41.8	59.6

a
Indicates that the algorithm gives no-solution [21].

$$\text{percentage error in time delay} = \frac{\text{measured time delay} - \text{theoretical time delay}}{\text{theoretical time delay}} \times 100 \quad (22)$$

The PD-source location is recalculated for the time-delay-groups TD-3 and TD-4, by using the non-iterative method and the iterative method (Newton's method). They are shown in Table 4. When the results are reproduced by using the non-iterative method, it is found that the solutions are complex numbers. However, in published literature [24], only the real part of the complex solution has been reported as the PD location. The PD source that is located by using the least-square algorithm has been reported in [24]. This is also given in Table 4. In Table 4 'a' indicates that the algorithm gives no-solution. It can be inferred from Table 4 that: (i) the non-iterative method gives a complex solution for the time-delay-groups TD-3 and TD-4; (ii) Newton's method gives a false PD location for the time-delay-groups TD-3 and TD-4; and (iii) the least-square algorithm gives no-solution for the time-delay-group TD-3 and an erroneous location for TD-4.

4 Conclusion

When invalid groups of time delays are used for a PD-source-localisation:

(a) The non-iterative method will give a complex solution.

(b) The iterative methods will fail to converge and they will not give any solution as the tolerance specified in the stopping criteria cannot be satisfied. When tolerance is not the only stopping criteria, solutions are obtained when the other criteria such as the time limit or the maximum number of iterations are reached. However, this results in a false PD-source-localisation.

Two methods for identifying such invalid 'time-delay-groups', which result in the solution of the system of the non-linear equations in the complex-number-field are reported. The suggested methods are:

- (i) Checking the sign of the function value of the proposed function.
- (ii) Checking the multiple sign changes of the Jacobian-determinant in the iterations of Newton's method.

The proposed methods have been validated by using the data taken from the published literature.

The initial checking of time-delay-groups that is proposed is important, in order to avoid the false location detection of a PD source. After identifying such time-delay-group, discarding it will significantly improve the accuracy of the statistical PD-source-localisation. This is irrespective of the algorithm that has been used for the PD-source-localisation.

5 Acknowledgments

Authors thank the National Institute of Technology Karnataka (NITK) for the support and encouragement, NITK in turn being supported by MHRD Government of INDIA. Authors thank the anonymous reviewers for their valuable suggestions.

6 References

- [1] Stone, G.C.: 'Partial discharge. VII. Practical techniques for measuring PD in operating equipment', *IEEE Electr. Insul. Mag.*, 1991, **7**, (4), pp. 9–19, doi: 10.1109/57.87656
- [2] Transformers Committee: 'IEEE guide for the detection and location of acoustic emissions from partial discharges in oil-immersed power transformers and reactors'. IEEE Std. C57.127-2007 (Revision of IEEE Std. C57.127-2000), 2007, pp. C1–47, doi: 10.1109/IEEESTD.2007.4293265
- [3] Lundgaard, L.E.: 'Partial discharge. XIII. Acoustic partial discharge detection-fundamental considerations', *IEEE Electr. Insul. Mag.*, 1992, **8**, (4), pp. 25–31, doi: 10.1109/57.145095
- [4] Lundgaard, L.E.: 'Partial discharge. XIV. Acoustic partial discharge detection-practical application', *IEEE Electr. Insul. Mag.*, 1992, **8**, (5), pp. 34–43, doi: 10.1109/57.156943
- [5] Eleftherion, P.M.: 'Partial discharge. XXI. Acoustic emission based PD source location in transformers', *IEEE Electr. Insul. Mag.*, 1995, **11**, (6), pp. 22–26, doi: 10.1109/57.475905
- [6] Hooshmand, R.A., Parastegari, M., Yazdanpanah, M.: 'Simultaneous location of two partial discharge sources in power transformers based on acoustic emission using the modified binary partial swarm optimisation algorithm', *IET Sci. Meas. Technol.*, 2013, **7**, (2), pp. 119–127, doi: 10.1049/iet-smt.2012.0029
- [7] Chan, J.C., Ma, H., Saha, T.K.: 'Hybrid method on signal de-noising and representation for online partial discharge monitoring of power transformers at substations', *IET Sci. Meas. Technol.*, 2015, **9**, (7), pp. 890–899, doi: 10.1049/iet-smt.2014.0358
- [8] Bua-Nunez, I., Posada-Roman, J.E., Rubio-Serrano, J., et al.: 'Instrumentation system for location of partial discharges using acoustic detection with piezoelectric transducers and optical fiber sensors', *IEEE Trans. Instrum. Meas.*, 2014, **63**, (5), pp. 1002–1013, doi: 10.1109/TIM.2013.2286891
- [9] Mirzaei, H., Akbari, A., Gockenbach, E., et al.: 'Advancing new techniques for UHF PD detection and localization in the power transformers in the factory tests', *IEEE Trans. Dielectr. Electr. Insul.*, 2015, **22**, (1), pp. 448–455, doi: 10.1109/TDEI.2014.004249
- [10] Akbari, A., Werle, P., Akbari, M., et al.: 'Challenges in calibration of the measurement of partial discharges at ultrahigh frequencies in power transformers', *IEEE Electr. Insul. Mag.*, 2016, **32**, (2), pp. 27–34, doi: 10.1109/MEI.2016.7414228
- [11] Sinaga, H.H., Phung, B.T., Blackburn, T.R.: 'Partial discharge localization in transformers using UHF detection method', *IEEE Trans. Dielectr. Electr. Insul.*, 2012, **19**, (6), pp. 1891–1900, doi: 10.1109/TDEI.2012.6396945
- [12] Kraetge, A., Hoek, S., Koch, M., et al.: 'Robust measurement, monitoring and analysis of partial discharges in transformers and other HV apparatus', *IEEE Trans. Dielectr. Electr. Insul.*, 2013, **20**, (6), pp. 2043–2051, doi: 10.1109/TDEI.2013.6678852
- [13] Boczar, T., Cichon, A., Borucki, S.: 'Diagnostic expert system of transformer insulation systems using the acoustic emission method', *IEEE Trans. Dielectr. Electr. Insul.*, 2014, **21**, (2), pp. 854–865, doi: 10.1109/TDEI.2013.004126
- [14] Chen, H.-C.: 'Partial discharge identification system for high-voltage power transformers using fractal feature-based extension method', *IET Sci. Meas. Technol.*, 2013, **7**, (2), pp. 77–84, doi: 10.1049/iet-smt.2012.0078
- [15] Gu, F.-C., Chang, H.-C., Chen, F.-H., et al.: 'Application of the Hilbert–Huang transform with fractal feature enhancement on partial discharge recognition of power cable joints', *IET Sci. Meas. Technol.*, 2012, **6**, (6), pp. 440–448, doi: 10.1049/iet-smt.2011.0213
- [16] Wu, M., Cao, H., Cao, J., et al.: 'An overview of state-of-the-art partial discharge analysis techniques for condition monitoring', *IEEE Electr. Insul. Mag.*, 2015, **31**, (6), pp. 22–35, doi: 10.1109/MEI.2015.7303259
- [17] Rubio-Serrano, J., Rojas-Moreno, M.V., Posada, J., et al.: 'Electro-acoustic detection, identification and location of partial discharge sources in oil–paper insulation systems', *IEEE Trans. Dielectr. Electr. Insul.*, 2012, **19**, (5), pp. 1569–1578, doi: 10.1109/TDEI.2012.6311502
- [18] Boya, C., Ruiz-Llata, M., Posada, J., et al.: 'Identification of multiple partial discharge sources using acoustic emission technique and blind source separation', *IEEE Trans. Dielectr. Electr. Insul.*, 2015, **22**, (3), pp. 1663–1673, doi: 10.1109/TDEI.2015.7116363
- [19] Harbaji, M., Shaban, K., El-Hag, A.: 'Classification of common partial discharge types in oil–paper insulation system using acoustic signals', *IEEE Trans. Dielectr. Electr. Insul.*, 2015, **22**, (3), pp. 1674–1683, doi: 10.1109/TDEI.2015.7116364
- [20] Woon, W.L., El-Hag, A., Harbaji, M.: 'Machine learning techniques for robust classification of partial discharges in oil–paper insulation systems', *IET Sci. Meas. Technol.*, 2016, **10**, (3), pp. 221–227, doi: 10.1049/iet-smt.2015.0076

- [21] Lu, Y., Tan, X., Hu, X.: 'PD detection and localisation by acoustic measurements in an oil-filled transformer', *IEE Proc., Sci. Meas. Technol.*, 2000, **147**, (2), pp. 81–85, doi: 10.1049/ip-smt:20000223
- [22] Markalous, S., Tenbohlen, S., Feser, K.: 'Detection and location of partial discharges in power transformers using acoustic and electromagnetic signals', *IEEE Trans. Dielectr. Electr. Insul.*, 2008, **15**, (6), pp. 1576–1583, doi: 10.1109/TDEI.2008.4712660
- [23] Tang, J., Xie, Y.: 'Partial discharge location based on time difference of energy accumulation curve of multiple signals', *IET Electr. Power Appl.*, 2011, **5**, (1), pp. 175–180, doi: 10.1049/iet-epa.2010.0029
- [24] Kundu, P., Kishore, N.K., Sinha, A.K.: 'A non-iterative partial discharge source location method for transformers employing acoustic emission techniques', *Appl. Acoust.*, 2009, **70**, (11–12), pp. 1378–1383, doi: 10.1016/j.apacoust.2009.07.001
- [25] Harrold, R.T.: 'Acoustical technology applications in electrical insulation and dielectrics', *IEEE Trans. Electr. Insul.*, 1985, **EI-20**, (1), pp. 3–19, doi: 10.1109/TEI.1985.348751
- [26] Howells, E., Norton, E.: 'Parameters affecting the velocity of sound in transformer oil', *IEEE Trans. Power Appar. Syst.*, 1984, **PAS-103**, (5), pp. 1111–1115, doi: 10.1109/TPAS.1984.318719
- [27] Al-Masri, W.M.F., Abdel-Hafez, M.F., El-Hag, A.H.: 'A novel bias detection technique for partial discharge localization in oil insulation system', *IEEE Trans. Instrum. Meas.*, 2016, **65**, (2), pp. 448–457, doi: 10.1109/TIM.2015.2482259
- [28] Kincaid, D., Cheney, E.W.: 'Numerical analysis: mathematics of scientific computing' (Brooks/Cole, Pacific Grove, CA, USA, 1991)
- [29] Hirsch, M.W., Smale, S., Devaney, R.L., et al.: 'Differential equations, dynamical systems, and an introduction to chaos' (Academic Press, San Diego CA, USA, 2004, 2nd edn.)
- [30] Padovan, J., Arechaga, T.: 'Formal convergence characteristics of elliptically constrained incremental Newton–Raphson algorithms', *Int. J. Eng. Sci.*, 1982, **20**, (10), pp. 1077–1097, doi: 10.1016/0020-7225(82)90091-X

7 Appendix

The PD source is located by solving the system of non-linear sphere equations

$$(x - x_1)^2 + (y - y_1)^2 + (z - z_1)^2 = (vT)^2 \quad (23)$$

$$(x - x_2)^2 + (y - y_2)^2 + (z - z_2)^2 = \{v(T + \tau_{12})\}^2 \quad (24)$$

$$(x - x_3)^2 + (y - y_3)^2 + (z - z_3)^2 = \{v(T + \tau_{13})\}^2 \quad (25)$$

$$(x - x_4)^2 + (y - y_4)^2 + (z - z_4)^2 = \{v(T + \tau_{14})\}^2 \quad (26)$$

Any two of the spheres intersect in a plane and the source can be located on this intersecting plane. The equation of the plane formed by the intersection of two spheres can be obtained by taking the difference of the corresponding sphere equations.

Three planes are obtained by taking the difference of (23) and (24), (23) and (25), and (23) and (26), respectively, and they are given in (27)–(29)

$$2(x_1 - x_2)x + 2(y_1 - y_2)y + 2(z_1 - z_2)z - 2v^2t_{12}T = x_1^2 - x_2^2 + y_1^2 - y_2^2 + z_1^2 - z_2^2 + v^2t_{12}^2 \quad (27)$$

$$2(x_1 - x_3)x + 2(y_1 - y_3)y + 2(z_1 - z_3)z - 2v^2t_{13}T = x_1^2 - x_3^2 + y_1^2 - y_3^2 + z_1^2 - z_3^2 + v^2t_{13}^2 \quad (28)$$

$$2(x_1 - x_4)x + 2(y_1 - y_4)y + 2(z_1 - z_4)z - 2v^2t_{14}T = x_1^2 - x_4^2 + y_1^2 - y_4^2 + z_1^2 - z_4^2 + v^2t_{14}^2 \quad (29)$$

From the plane (27)–(29), the unknown variable T has to be eliminated. The equation for T is obtained in terms of x , y , and z from (27) and is given in (30) (see (30)). By substituting (30) in (28) and (29), we get two plane equations (31) and (32)

$$2x\sigma_1 + 2y\sigma_3 + 2z\sigma_5 = \sigma_8 \quad (31)$$

$$T = \frac{2(x_1 - x_2)x + 2(y_1 - y_2)y + 2(z_1 - z_2)z - x_1^2 + x_2^2 - y_1^2 + y_2^2 - z_1^2 + z_2^2 - v^2t_{12}^2}{2v^2t_{12}} \quad (30)$$

$$2x\sigma_2 + 2x\sigma_4 + 2z\sigma_6 = \sigma_9 \quad (32)$$

where [these are the constants given in the body of this paper forming (2)–(10)]

$$\begin{aligned} \sigma_1 &= \frac{(x_1 - x_2)}{2t_{12}v^2} - \frac{(x_1 - x_3)}{2t_{13}v^2} \\ \sigma_2 &= \frac{(x_1 - x_2)}{2t_{12}v^2} - \frac{(x_1 - x_4)}{2t_{14}v^2} \\ \sigma_3 &= \frac{(y_1 - y_2)}{2t_{12}v^2} - \frac{(y_1 - y_3)}{2t_{13}v^2} \\ \sigma_4 &= \frac{(y_1 - y_2)}{2t_{12}v^2} - \frac{(y_1 - y_4)}{2t_{14}v^2} \\ \sigma_5 &= \frac{(z_1 - z_2)}{2t_{12}v^2} - \frac{(z_1 - z_3)}{2t_{13}v^2} \\ \sigma_6 &= \frac{(z_1 - z_2)}{2t_{12}v^2} - \frac{(z_1 - z_4)}{2t_{14}v^2} \\ \sigma_7 &= \frac{t_{12}^2v^2 + x_1^2 - x_2^2 + y_1^2 - y_2^2 + z_1^2 - z_2^2}{2t_{12}v^2} \\ \sigma_8 &= \sigma_7 - \frac{t_{13}^2v^2 + x_1^2 - x_3^2 + y_1^2 - y_3^2 + z_1^2 - z_3^2}{2t_{13}v^2} \\ \sigma_9 &= \sigma_7 - \frac{t_{14}^2v^2 + x_1^2 - x_4^2 + y_1^2 - y_4^2 + z_1^2 - z_4^2}{2t_{14}v^2} \end{aligned}$$

Two planes intersect in a line and the PD source can be located on this line. The equation of the line formed by the intersection of two planes given in (31) and (32) are obtained as follows.

Let \mathbf{P} be a vector parallel to the required line, then

$$\mathbf{P} = \begin{vmatrix} \hat{i} & \hat{j} & \hat{k} \\ 2\sigma_1 & 2\sigma_3 & 2\sigma_5 \\ 2\sigma_2 & 2\sigma_4 & 2\sigma_6 \end{vmatrix}$$

$$\mathbf{P} = \hat{i}(4\sigma_3\sigma_6 - 4\sigma_5\sigma_4) - \hat{j}(4\sigma_1\sigma_6 - 4\sigma_2\sigma_5) + \hat{k}(4\sigma_1\sigma_4 - 4\sigma_2\sigma_3)$$

$$x_0 = 4\sigma_{11} \quad (33)$$

$$y_0 = -4\sigma_{10} \quad (34)$$

$$z_0 = 4\sigma_{12} \quad (35)$$

where [these are the constants given in the body of this paper forming (11)–(13)]

$$\sigma_{10} = \sigma_1\sigma_6 - \sigma_2\sigma_5$$

$$\sigma_{11} = \sigma_3\sigma_6 - \sigma_4\sigma_5$$

$$\sigma_{12} = \sigma_1\sigma_4 - \sigma_2\sigma_3$$

The point (x_1, y_1, z_1) on the line can be located at $z=0$ plane. Thus, substitute $z=0$ in the plane (31) and (32) to get (x_1, y_1, z_1) given in (36)–(38)

$$x_1 = \frac{\sigma_{14}}{\sigma_{15}} \quad (36)$$

$$y_1 = \frac{-\sigma_{13}}{\sigma_{15}} \quad (37)$$

$$z_1 = 0 \quad (38)$$

where [these are the constants given in the body of this paper forming (14)–(16)]

$$\sigma_{13} = \sigma_2\sigma_8 - \sigma_1\sigma_9$$

$$\sigma_{14} = \sigma_4\sigma_8 - \sigma_3\sigma_9$$

$$\sigma_{15} = 2(\sigma_1\sigma_4 - \sigma_2\sigma_3)$$

The equation of the line formed by the intersection of two planes given in (31) and (32) is given in (39)

$$\frac{x - (\sigma_{14}/\sigma_{15})}{(\sigma_{11}/\sigma_{12})} = \frac{y + (\sigma_{13}/\sigma_{15})}{(-\sigma_{10}/\sigma_{12})} = z = A \quad (39)$$

From (39), any point on the line (x, y, z) can be obtained and is given in (40)–(42), respectively

$$x = \frac{\sigma_{11}}{\sigma_{12}}A + \frac{\sigma_{14}}{\sigma_{15}} \quad (40)$$

$$y = \frac{-\sigma_{10}}{\sigma_{12}}A - \frac{\sigma_{13}}{\sigma_{15}} \quad (41)$$

$$z = A \quad (42)$$

The value of T is obtained in terms of A by substituting (40)–(42) in (30)

$$T = \frac{2A\sigma_{16} - \sigma_{17}}{2v^2t_{12}} \quad (43)$$

where [these are the constants given in the body of this paper forming (17) and (18)]

$$\sigma_{16} = z_1 - z_2 - \frac{\sigma_{10}(y_1 - y_2)}{\sigma_{12}} + \frac{\sigma_{11}(x_1 - x_2)}{\sigma_{12}}$$

$$\begin{aligned} \sigma_{17} &= t_{12}^2v^2 + x_1^2 - x_2^2 + y_1^2 - y_2^2 + z_1^2 - z_2^2 \\ &+ \frac{2\sigma_{13}(y_1 - y_2)}{\sigma_{15}} - \frac{2\sigma_{14}(x_1 - x_2)}{\sigma_{15}} \end{aligned}$$

The line intersects any one of the spheres in two points, resulting in a quadratic equation. To find the quadratic equation formed by the intersection of line given in (39) and sphere given in (23), (40)–(43) are substituted in (23). The resulting quadratic equation in variable A is given in (44)

$$\begin{aligned} &A^2 \left[\left(\frac{\sigma_{10}}{\sigma_{12}} \right)^2 + \left(\frac{\sigma_{11}}{\sigma_{12}} \right)^2 - \frac{\sigma_{16}^2}{t_{12}^2v^2} + 1 \right] \\ &+ A \left[2z_1 - \frac{2\sigma_{10}\sigma_{18}}{\sigma_{12}} + \frac{2\sigma_{11}\sigma_{19}}{\sigma_{12}} - \frac{\sigma_{16}\sigma_{17}}{t_{12}^2v^2} \right] \\ &+ \left[\sigma_{18}^2 + \sigma_{19}^2 + z_1^2 - \frac{\sigma_{17}^2}{4t_{12}^2v^2} \right] = 0 \end{aligned} \quad (44)$$

where [these are the constants given in the body of this paper forming (19) and (20)]

$$\sigma_{18} = y_1 + \frac{\sigma_{13}}{\sigma_{15}}$$

$$\sigma_{19} = x_1 - \frac{\sigma_{14}}{\sigma_{15}}$$

The nature of the roots of a quadratic equation can be identified from its discriminant value. Therefore, the discriminant of (44) is chosen as a function F given in (45) to identify whether the solution lies in the real-number-field or in the complex-number-field. This is (21) given in the body of this paper for function F

$$F = \left[2z_1 - \frac{2\sigma_{10}\sigma_{18}}{\sigma_{12}} + \frac{2\sigma_{11}\sigma_{19}}{\sigma_{12}} - \frac{\sigma_{16}\sigma_{17}}{t_{12}^2 v^2} \right]^2 - \left[\sigma_{18}^2 + \sigma_{19}^2 + z_1^2 - \frac{\sigma_{17}^2}{4t_{12}^2 v^2} \right] \left[4 \left(\frac{\sigma_{10}}{\sigma_{12}} \right)^2 + 4 \left(\frac{\sigma_{11}}{\sigma_{12}} \right)^2 - \frac{4\sigma_{16}^2}{t_{12}^2 v^2} + 4 \right] \quad (45)$$